ELSEVIER

Polymer 40 (1999) 2129–2137

polymer

Mixtures of numerous different *n*-alkanes: 2. Studies by X-ray diffraction and differential thermal analyses with increasing temperature

V. Chevallier, D. Petitjean, M. Bouroukba, M. Dirand*

Laboratoire de Thermodynamique des Séparations, Ecole Nationale Supérieure des Industries Chimiques, Institut National Polytechnique de Lorraine, 1 rue Grandville BP 451-1, F54001, Nancy cedex, France

Received 17 March 1998; revised 13 May 1998; accepted 13 May 1998

Abstract

The structural behaviour of the orthorhombic multi-*n*-alkane crystalline β' phase, observed in mixtures consisting of 23 ($19 < n < 43$) and 33 ($19 < n < 53$) *n*-alkanes respectively, is studied by X-ray diffraction with increasing temperature. A Rotator single-phase domain of rhombohedral (or hexagonal) α-RII type is observed below the solidus point. The product, consisting of 23 *n*-alkanes, undergoes this structural transition ($\beta' \rightarrow \alpha$-RII) through two two-phase domains: first, a region with the β' and β(Fmmm) phases; then, a domain with the two β(Fmmm)-RI and α(R$\bar{3}$m)-RII Rotator phases. For two β' solid solutions consisting of 33 *n*-alkanes, a single two-phase domain ($\beta' + \alpha$-RII) is observed in the course of this structural crystal–Rotator transition.

Keywords: *n*-alkanes; Multi-*n*-alkane solid solution; Rotator phases

1. Introduction

According to experiments carried out in our laboratory [1], a single orthorhombic solid solution was highlighted in complicated mixtures of numerous consecutive *n*-alkanes (hereafter denoted by C_n) at 'room' temperature. The structure of this multi-C_n phase, consisting of 23 ($19 < n < 43$) or 33 C_n ($19 < n < 53$) respectively, is identical to one of the two orthorhombic intermediate solid solutions which have been observed in binary [2–11] and ternary[12,13] molecular alloys of consecutive C_n and called β_n' and β_n''.

Like the orthorhombic odd-numbered pure C_{2p+1} and the intermediate β_n' and β_n'' phases of binary mixtures of C_n [2–11], this multi-C_n solid solution presents a lamellar structure of molecule layer stacking: the stacking identity long *c* period of this lamellar structure corresponds to a chain length of a hypothetical orthorhombic C_n whose carbon atom number is quasi-equal to the average carbon atom number of the multi-C_n mixtures [1].

The aim of this study is to determine the multi-C_n product behaviour with increasing temperature and to compare it with that of the β_n' and β_n'' intermediate phases of binary mixtures.

2. Structural behaviour of orthorhombic intermediate solid solutions versus temperature

The intermediate solid solutions, which have been observed in all the binary and ternary mixtures of C_n [2–13] ($19 < n < 27$), are isostructural with two phases only, called β_n' and β_n''. These intermediate β_n' and β_n'' phases present orthorhombic unit cells (Fig. 1a and b), whose space groups have not yet been precisely determined [2,3,5,8]. The index $n = 1$ or 2 allows the identification of isostructural phases of different stoïchiometries on both sides of the middle intermediate solid solution in the same binary or ternary system.

With increasing temperature, all the β_n' and β_n'' solid solutions undergo the same solid–solid transitions as the orthorhombic pure C_{23} or C_{25} [14–17] above their δ transition[18] up to their melting point [9,11,19–31] (Fig. 1), for reminder:

$$\beta_n' \text{ and } \beta_n'' \rightarrow \beta(\text{Fmmm}) \Rightarrow \beta - \text{RI(Fmmm)} \rightarrow \alpha - \text{RII(R}\bar{3}\text{m)} \rightarrow \text{liquid}$$

where $\rightarrow$ denotes first-order transition, and $\Rightarrow$ denotes higher-order transition.

1. The occurence of the β(Fmmm) phase is accompanied by:

* Corresponding author.

0032-3861/99/$ - see front matter
PII: S0032-3861(98)00409-1

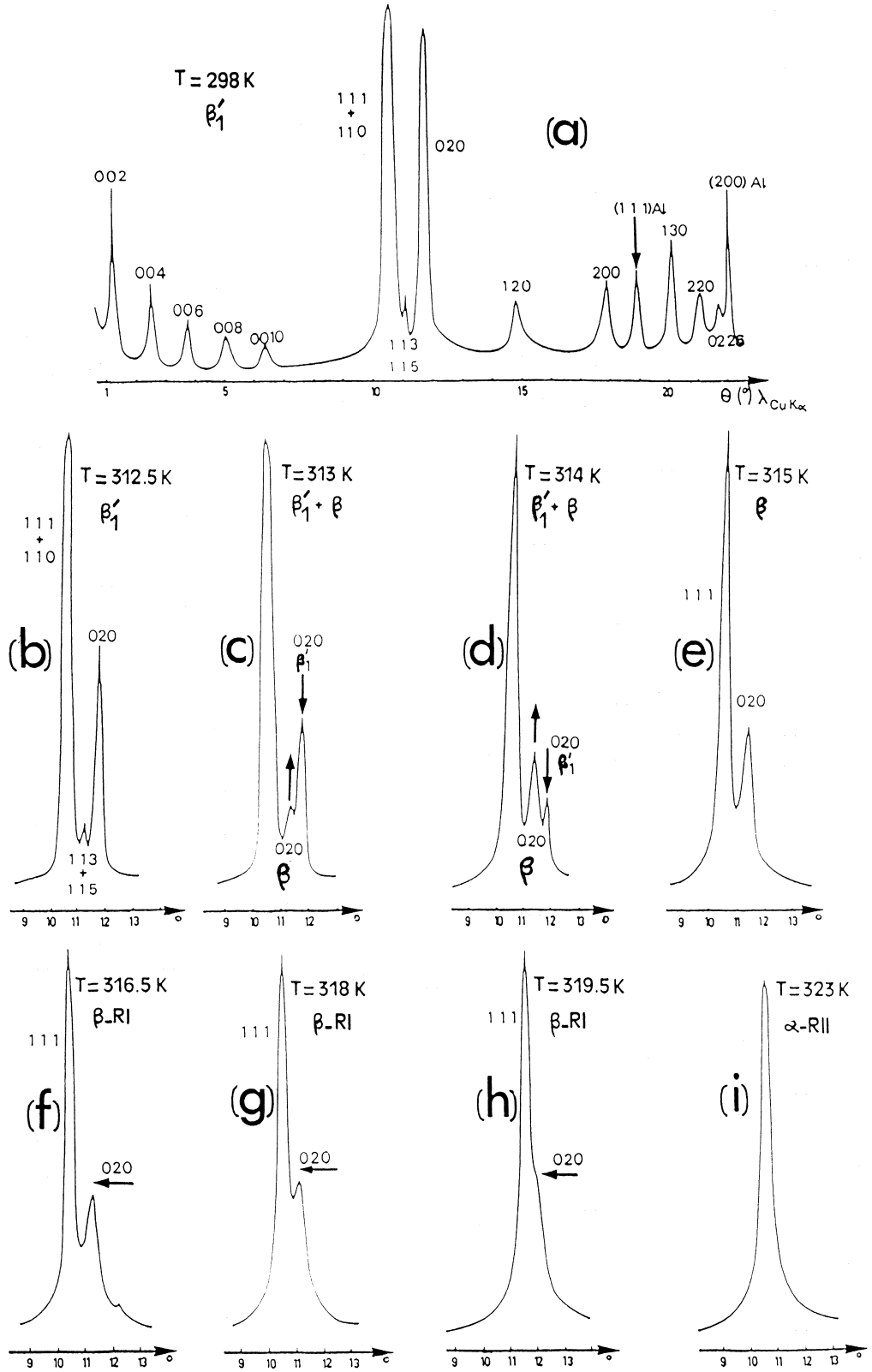

Fig. 1. Structural evolutions with increasing temperature from the intermediate β_1' solid solution of C_{24}/10 mol% C_{26} mixture up to the α-RII Rotator phase.

- the disappearance of all the diffraction peaks (*h k l*) whose indices have not the same parity [19–27];
- an important shift of the (0 2 0) diffraction towards small Bragg angles, that corresponds to an increase of crystallographic *b* parameter and of the unit cell base area (*a*,*b*) (Fig. 1c, d and e).At the first, the β(Fmmm) phase does not undergo any crystalline parameter evolution in a small temperature range; then, the

crystallographic parameter b/a ratio of this phase increases progressively: the beginning of the phenomenon is observed by X-ray diffraction when the (0 2 0) line moves toward the (1 1 1) diffraction peak (Fig. 1f, g and h); however, the X-ray diffraction line intensities do not change significantly and the appearance of a second phase, which characterizes a first-order transition in the binary systems, is not seen. This phenomenon, which is accompanied by an abnormal and continuous enthalpy consumption without change of the space group (Fmmm) of the crystallographic structure and the composition of this β phase, does not obey Gibb's phase law concerning first-order transitions and probably corresponds to a second-order transition, which characterizes the RI Rotator state of this β(Fmmm) phase, as was highlighted by Ungar [14] and Ungar and Masic [15] for the pure C_{23}.

2. When the two (0 2 0) and (1 1 1) diffraction lines coincide (Fig. 1i), the symmetry of the unit cell base (a,b) becomes hexagonal ($b/a = \sqrt{3}$) and the mixtures undergo a further weak first-order transition into the rhombohedral α-RII Rotator phase whose space group $R\bar{3}m$ has been determined by Ungar [14] and Ungar and Masic [15]: the stacking mode of the chains along the crystallographic long c axis corresponds to the rhombohedral ABCABC sequence of cristalline planes instead of the orthorhombic (or hexagonal) ABABAB sequence as in the orthorhombic β(Fmmm) structure [14–17].

NB: when the temperature increases, the crystalline phases of the even-numbered C_{2p}, whose structures are triclinic or monoclinic ($2p < 38$), undergo a single crystal–Rotator transition with the appearance of the α-RII phase only or of another Rotator phase, denoted RIII, RIV, RV [16,17,32–34]; but at the equilibrium state, the orthorhombic β(Fmmm) phase are not observed in the triclinic even-numbered pure C_{2p}, nor in the RI Rotator state.

3. Experimental

C_ns were purchased from Aldrich Chemical Company: their purity grade is 99 mol% as determined by gas chromatography. The binary mixture (C_{24}/10 mol% C_{26}) was prepared by weighing together the solid components, melting

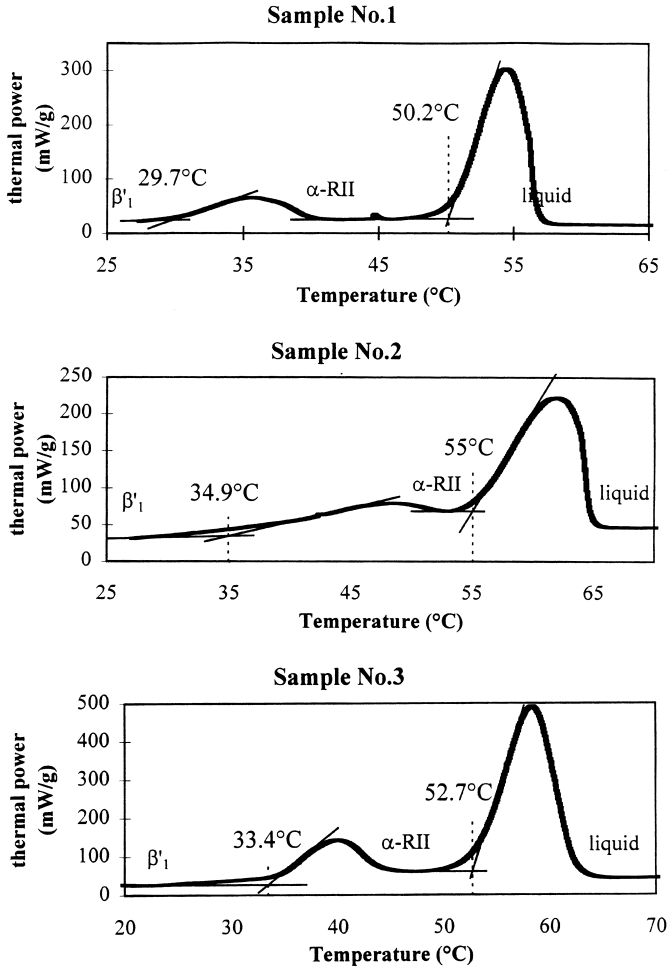

Fig. 2. DTA curves of multi-C_n mixtures 1–3: temperature of solid–solid transition beginning and of solidus point, according to the conventional scheme.

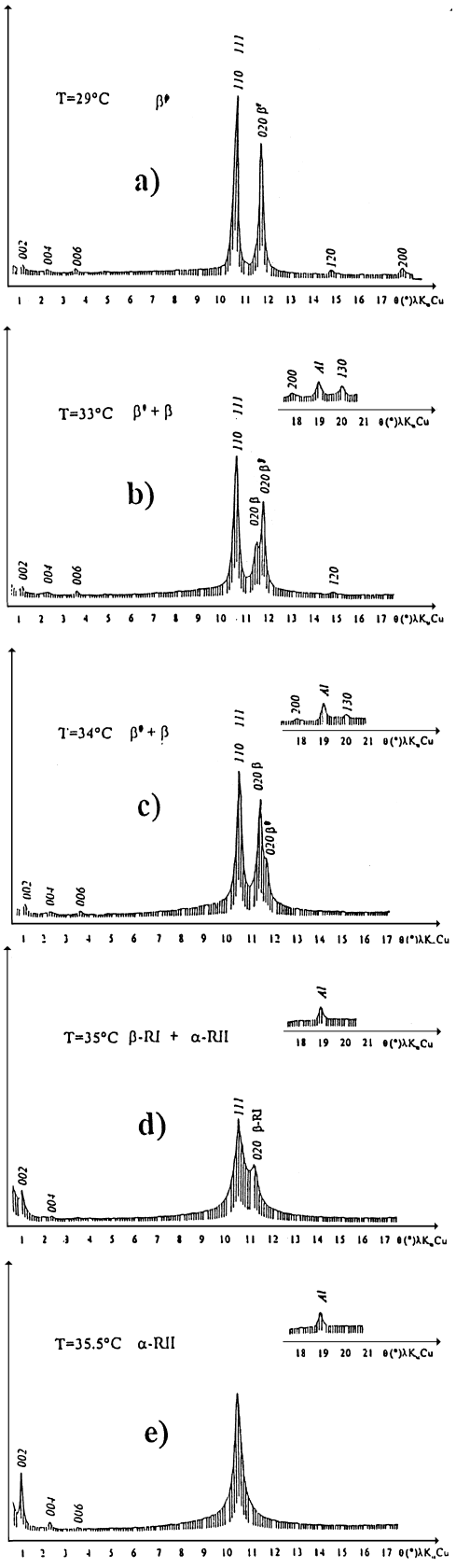

Fig. 3. Structural evolutions of the multi-C_n β' solid solution of Sample 1, consisting of 23 C_ns ($19 < n < 43$): observation of two two-phase domains in the course of the solid–Rotator transition; first ($\beta' + \beta$(Fmmm)), then (β-RI(Fmmm) + α-RII ($R\bar{3}m$)).

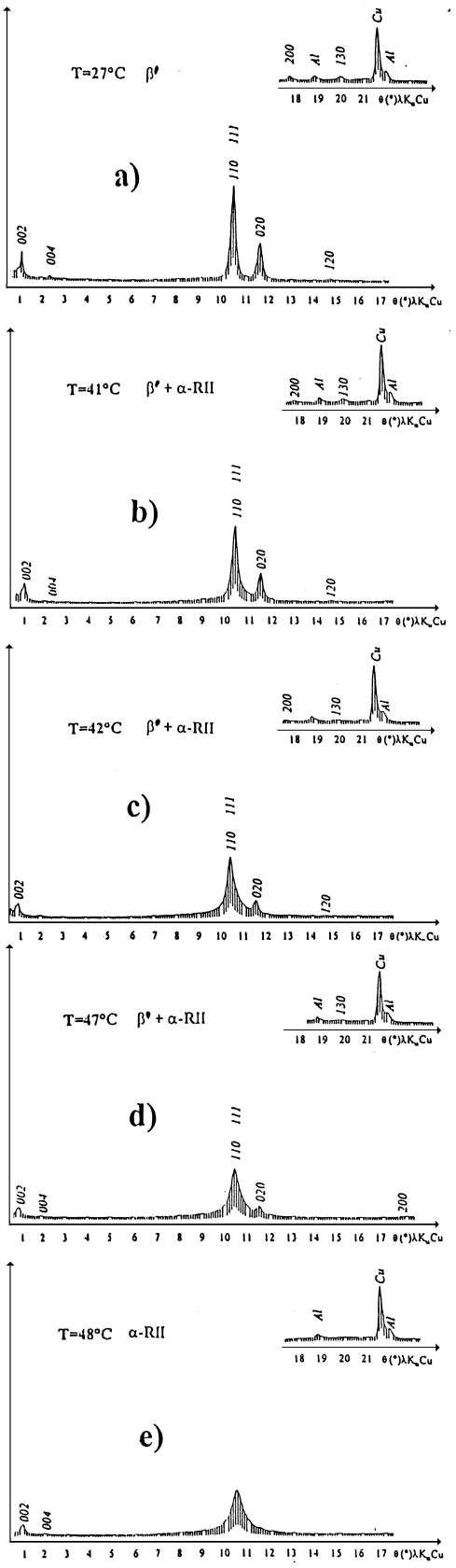

Fig. 4. Structural evolutions of the multi-C_n β' solid solution of Sample 2, consisting of 33 C_ns ($19 < n < 53$): observation of the orthorhombic–Rotator transition ($\beta' \rightarrow \alpha$-RII) through a single two–phase domain ($\beta' + \alpha$-RII).

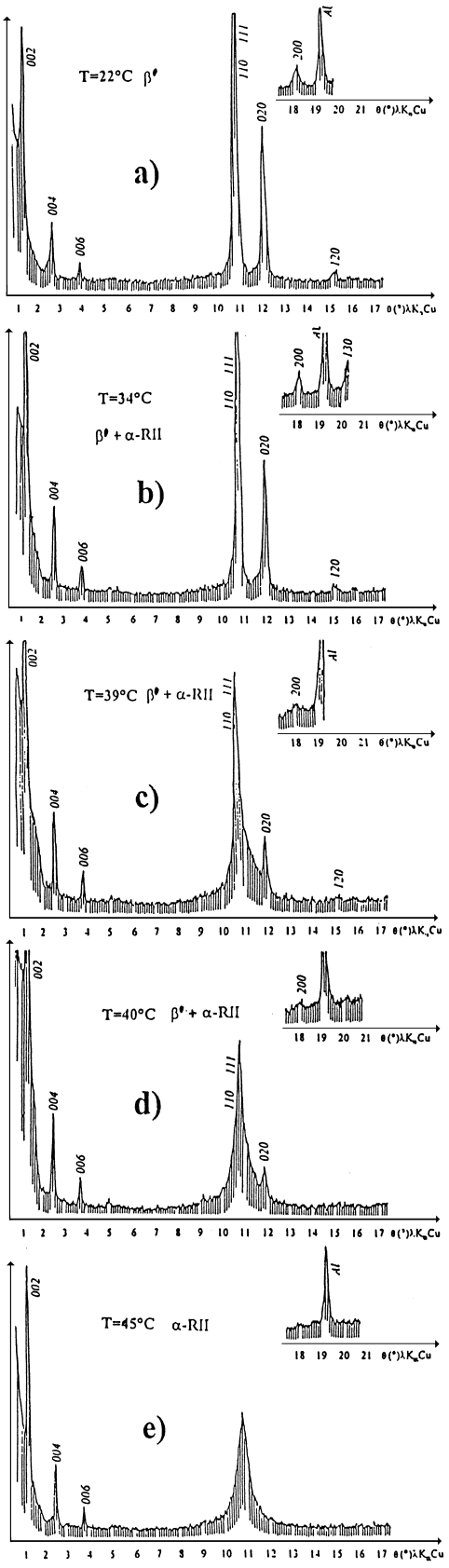

Fig. 5. Structural evolutions of the multi-C_n β' solid solution of 50–50 wt% 3 of commercial products 1 and 2: observation of the orthorhombic–Rotator transition ($\beta' \rightarrow \alpha$-RII) through a single two-phase domain ($\beta' + \alpha$-RII).

and thorough mixing. The homogeneous liquid solution thus obtained was quenched in a crystallizing dish maintained at a low temperature in a Dewar vessel filled with liquid air. Such rapid cooling ensured an uniform steric concentration of each component in the mixture.

X-ray diffraction experiments were carried out on powder samples using $\lambda_{K\alpha}$ copper radiation. The X-ray diffractograms were obtained with a CGR diffractometer (Theta 60) and the X-ray diffraction analyses were performed at different temperatures with the help of a heated sample holder; heating or cooling of the sample holder was based on the Peltier effect: the precision of the sample temperature was within $\pm$ 0.2 K of the set point. The focused monochromatic beam was obtained with a filament intensity of 10 mA at 48 kV and the line positions were measured with an accuracy of 0.05° for each value of Bragg angles; the calibration was done with pure aluminium as standard, of which the sample holder was made.

The differential thermal analyses (DTAs) were performed using a Setaram DSC111 calorimeter of the Tian Calvet type. The samples, preliminary melted and cooled in the measuring crucible, were heated from room temperature to above the liquidus point at a rate of 0.5 K min^{-1}. The temperature of transition peaks are determined as defined on Fig. 2 with a precision of $\pm$0.5 K.

Four samples have been studied, with the following numbering:

1. Samples 1 and 2: two commercial products, purchased from Prolabo, respectively called paraffin 52–54°C and 60–62°C in its commercial catalogue.
2. Sample 3: a 50–50 wt% mixture of the two commercial products (Sample 1 + Sample 2).The X-ray analyses, carried out at 'room temperature' [1], have shown that these three multi-C_n mixtures (Samples 1–3) form a single solid solution identical to the orthorhombic intermediate β_n' phase of binary and ternary molecular alloys of C_n [2–13](Fig. 3a, Fig. 4a and Fig. 5a).
3. Sample 4: the binary mixture of C_{24}: 10 mol% C_{26} whose 'low temperature' phase is the orthorhombic intermediate β_1' solid solution [8,9].

The C_n concentrations of Samples 1–3 were determined by gas chromatography; they are shown in Table 1 and Fig. 6.

4. Results

On the one hand, the thermal accidents, which are observed on the DTA curves (Fig. 2), show a peak of solid–solid transition below the solidus point of the multi-C_n mixtures and indicate the temperature range of transformation equilibria (Table 2). On the other hand, this range was explored by X-ray diffraction analyses (Figs 3–5) to characterize the structural evolutions in the course of this solid–solid transition and to confirm the initial and final

Table 1
Mol% concentrations of multi-C_n Samples 1, 2 and 3: Sample 3 is a 50–50 wt% mixture of commercial products 1 and 2 and their molar fractions in mixture 3 are $x_3 = 0.576$ and $x_4 = 0.424$ respectively

	Sample 1 (mol%)	Sample 2 (mol%)	Sample 3 (mol%)
C20	0.070	0.038	0.056
C21	0.812	0.182	0.546
C22	4.778	0.678	3.046
C23	13.057	2.078	8.419
C24	20.360	4.254	13.556
C25	18.464	6.594	13.450
C26	14.594	8.476	12.009
C27	9.236	10.615	9.819
C28	6.568	11.756	8.760
C29	4.682	11.722	7.656
C30	3.351	10.376	6.318
C31	2.051	8.807	4.905
C32	1.050	6.702	3.438
C33	0.424	5.072	2.388
C34	0.198	3.572	1.623
C35	0.104	2.594	1.156
C36	0.062	1.831	0.809
C37	0.045	1.419	0.626
C38	0.030	1.039	0.456
C39	0.029	0.639	0.286
C40	0.014	0.489	0.215
C41	0.014	0.318	0.142
C42	0.007	0.246	0.108
C43	–	0.161	0.068
C44	–	0.113	0.048
C45	–	0.068	0.029
C46	–	0.058	0.025
C47	–	0.033	0.014
C48	–	0.024	0.010
C49	–	0.016	0.007
C50	–	0.015	0.006
C51	–	0.008	0.003
C52	–	0.007	0.003

temperatures of transition (Table 2). All the experiments have been carried out with increasing temperature at equilibrium state. At 'room temperature', the X-ray diffractograms of multi-C_n Samples 1–3 correspond to that of a single orthorhombic solid solution, identical to the β' phase of binary mixture 4.

4.1. Sample 1

Fig. 3 shows the structural evolutions of Sample 1, consisting of 23 C_ns ($19 < n < 43$), with increasing temperature. Above 29°C, a new diffraction line appears near the peak (0 2 0) towards the small Bragg angles (Fig. 3a); it indicates the occurrence of a new phase. From 29°C to 34.5°C, the intensity of this new line increases and that of the β' phase (0 2 0) peak decreases (Fig. 3b and c): in this temperature range, this observation characterizes a two-phase domain with the presence of the 'low temperature' multi-C_n β' solid solution and of the orthorhombic β(Fmmm) phase; indeed the intensities of diffraction lines, whose ($h\,k\,l$) indices do not have the same parity, progressively decrease. When the characteristic peaks of the β' phase have completely disappeared at a temperature of 34.5°C, the β-RI Rotator state is detected by a small gradual shift of the β(Fmmm) phase (0 2 0) diffraction line from 11.3° to 11° (λCuKα, Fig. 3d), but simultaneously the rhombohedral α-RII ($R\bar{3}m$) Rotator phase appears with the widening of the (1 1 1) peak. This two-Rotator phase domain is observed in a small temperature range, situated above 34.5°C up to 35.5°C; for the higher temperatures set below the melting point, the β-RI phase (0 2 0) diffraction line has disappeared and the diffractograms correspond to that of the single rhombohedral α-RII Rotator phase (Fig. 3e).

Table 2
Temperatures of solid–solid transition starts, determined by DTA (±0.5°C), and of transition end, observed by X-ray diffraction (±0.2°C) with increasing temperature

Sample	Two-phase domain		Solidus point (°C)
	$\beta' + \beta$(Fmmm)	β-RI + α-RII	
1	29.7–34.5°C	34.5–35.5°C	50.2
	$\beta' + \alpha$-RII		
2	34.9–48°C		55
3	33.4–44°C		52.7

4.2. Samples 2 and 3

Like the DTA curve observations (Fig. 2), the X-ray diffraction analyses (Figs 4 and 5) with increasing temperature reveal a single structural solid–solid transition for Samples 2 and 3, consisting of 33 C_ns ($19 < n < 53$).

1. When the temperature increases in the range of the first peak of DTA curves, the diffraction line intensities of the 'low temperature' orthorhombic multi-C_n β' phase, particularly the (1 1 0) + (1 1 1) and (0 2 0) peaks, progressively decrease without any significant variation of the Bragg angle values (Figs 4 and 5).
2. Jointly:

- for Sample 2, the diffraction line (1 1 0) + (1 1 1) becomes wider (Fig. 4b, c and d).
- for mixture 3 of two commercial products 1 and 2, a new diffraction line appears at the base of the (1 1 0) + (1 1 1) intense peak of the 'low temperature' orthorhombic multi-C_n β' phase with a higher Bragg angle (10.8° instead of 10.75°, λCuKα, Fig. 5b). The intensity of this new line, corresponding to the appearance of a new phase, increases according to temperature in this two-phase domain (Fig. 5b, c and d).

3. The structural transformation is finished when the orthorhombic β' phase (0 2 0) diffraction line has completely disappeared: the diffractograms, which are then obtained, are characteristic of a rhombohedral Rotator phase of α-RII type (Fig. 4e, Fig. 5e).

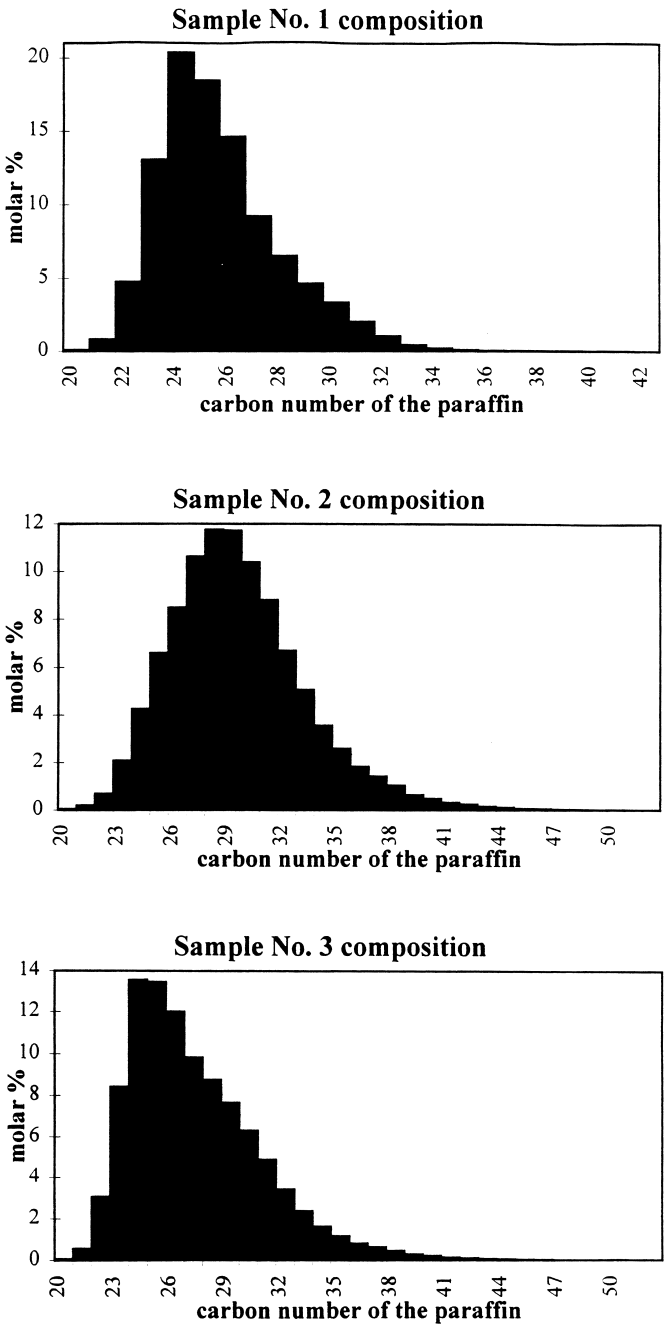

Fig. 6. Concentration distributions of C_n in commercial products 1–3.

NB:

- in the three cases, the positions of the diffraction lines (0 0 *l*) do not significantly evolve during this transition: the molecule stacking identity period does not change and thus the three multi-C_n mixtures also form a single α-RII Rotator solid solution at 'high temperature' below the solidus point;
- for multi-C_n products 2 and 3, consisting of 33 C_n, the peak (0 2 0) of the 'low temperature' orthorhombic β' solid solution does not significantly move in the course of this structural transformation: these two multi-C_n mixtures do not present the β(Fmmm) phase, nor the RI Rotator state with increasing temperature at the equilibrium state.

5. Conclusion

For Sample 1, consisting of 23 C_n ($19 < n < 43$), the solid–solid transition corresponds to two-phase domains with:

1. first, the presence of the 'low temperature' multi-C_n β' phase and the appearance of the β(Fmmm) phase;
2. then, the observation of both the β(Fmmm)-RI Rotator

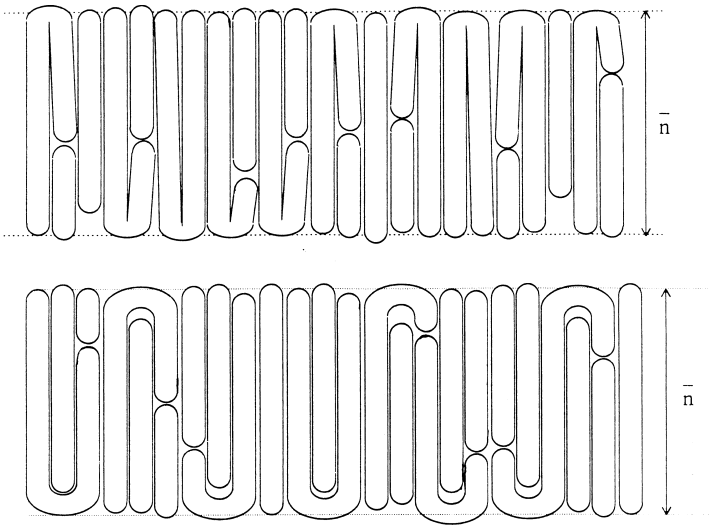

Fig. 7. Probable configurations of C_n molecules in a stacking layer of the multi-C_n β' or α-RII solid solutions: more accurate techniques must be used to confirm them.

phase and the rhombohedral α-RII Rotator phase when the 'low temperature' multi-C_n β' solid solution has completely disappeared. Finally below the solidus point this α-RII Rotator phase forms a single-phase domain.

Multi-C_n products 2 and 3, consisting of 33 C_ns, undergo a single crystal–Rotator transition in a temperature range which defines a two-phase domain with the presence of the 'low temperature' orthorhombic multi-C_n β' solid solution and the 'high temperature' rhombohedral Rotator phase of α-RII type ($R\bar{3}m$). Then this Rotator phase forms a single-phase region just below the solidus point.

The molecule stacking identity long *c* period does not significantly vary in the course of these orthorhombic–rhombohedral transformations. As in the 'low temperature' orthorhombic β' phase, these complex multi-C_n mixtures present a single Rotator solid solution of α-RII type at 'high temperature': the crystallographic long *c* parameter of this phase corresponds to a chain length of a hypothetical C_n whose carbon atom number is quasi-equal to the average carbon atom $\bar{n}$ number of multi C_n mixtures [1] (Fig. 7).

As in the orthorhombic structure of the 'low temperature' multi-C_n β' solid solution, the chains, whose carbon atom numbers are higher than that of this hypothetical C_n, must bend to insert themselves between the molecule layer stacking crystallographic planes (Fig. 7). It is difficult for these bent molecules to undergo the orientational oscillations around their long axis as described in the pure C_{23} RI-Rotator state by Craievich et al. [35]. That is the reason why this RI Rotator state is not seen in mixtures 2 and 3 or fleetingly observed in Sample 1; only the small molecules, which are rigid, may freely turn around their long axis in the α-RII Rotator phase, as also observed in the C_{23} α-RII Rotator phase from neutron scattering experiments by Craievich et al. [35].

In view of the tangle of all the molecules, this movement requires a lot of enthalpy (Fig. 2); thus, as for the triclinic even-numbered C_{2p} structure—where the molecule layers are very ordered—this rotation movement simultaneously appears with the coming of the rhombohedral α-RII Rotator phase. In all likelihood, the stability of molecule layers in the 'low temperature' orthorhombic multi-C_n β' solid solution of both Samples 2 and 3 is higher than that of the odd-numbered pure C_{2p+1} orthorhombic phase (Pbcm) in which all the molecules are rigid. The conformational disorder of chain stacking in the multi-C_n crystalline solid solutions, as described by Clavell-Grunbaum et al. [31], disturbs the interlamellar regions of molecule layers; however between these interface regions the longer chains, which bend, must find appropriate smaller partners. Thus the higher molecules are associated with the smaller ones, and so on (Fig. 7), to maintain a coherent molecule layer; the disorder in the interfacial planes generates a new order in molecule layers which improves the stability of this 'low temperature' orthorhombic multi-C_n solid solution in relation to that of the orthorhombic phase (Pbcm) of odd-numbered C_{2p+1}.

References

[1] Dirand M, Chevallier V, Provost E, Bourdet JB, Bouroukba M, Petitjean D. Polymer, in press.
[2] Smith AE. Acta Cryst 1957;10:802.
[3] Luth H, Nyburg SG, Robinson PM, G Scott H. Mol Cryst Liq Cryst 1974;27:337.
[4] Hasnaoui N, Dellacherie J, Schuffenecker L, Dirand M, Balesdent D. J Chim Phys 1988;85 (2):153.
[5] Gerson AR, Nyburg SC. Acta Cryst 1994;B50:252.
[6] Jouti B, Bourdet JB, Bouroukba M, Dirand M. Mol Cryst Liq Cryst 1995;270:159.
[7] Jouti B, Petitjean D, Provost E, Bouroukba M, Dirand M. J Mol Struct 1995;356:191.
[8] Achour-Boudjema Z, Bourdet JB, Petitjean D, Dirand M. J Mol Struct 1995;354:197.
[9] Dirand M, Achour Z, Jouti B, Sabour A, Gachon JC. Mol Cryst Liq Cryst 1996;275:293.

[10] Nouar H, Petitjean D, Bourdet JB, Dirand M. J Mol Struct 1997;415:2.
[11] Dirand M, Achour Z, Bourdet JB, Bouroukba M. Entropie (Vol. 202–203) 1997:41.
[12] Nouar H, Bouroukba M, Petitjean D, Dirand M. Mol Cryst Liq Cryst 1998;309:273.
[13] Nouar H, Petitjean D, Bouroukba M, Dirand M. Rev IFP 1998;53:27.
[14] Ungar G J Phys Chem 1983;87:689.
[15] Ungar G, Masic G. J Phys Chem 1985;80:1036.
[16] Doucet J, Denicolo I, Craievich AF, Germain G. J Chem Phys 1984;80 (4):1647.
[17] Doucet J, Dianoux AJ. J Chem Phys 1984;81 (11):5043.
[18] Snyder RG, Maroncelli AF, Qi SP, Strauss HL. Science 1981;214 (9):188.
[19] Hasnaoui N, Dellacherie J, Schuffenecker L, Dirand M. J Chim Phys 1988;85 (6):675.
[20] Achour Z, Bourdet JB, Bouroukba M, Dirand M. J Chim Phys 1993;90:325.
[21] Achour-Boudjema Z, Bouroukba M, Dirand M. Thermochimica Acta 1996;276:243.
[22] Jouti B, Provost E, Petitjean D, Bouroukba M, Dirand M. Mol Cryst Liq Cryst 1996;287:275.
[23] Dirand M, Achour-Boudjema Z. J Mol Struct 1996;375:243.
[24] Rejabalee F, Espeau P, Haget Y, Cuevas-Diarte MA. XXIth J.E.E.P., Rouen, 1995:294.
[25] Robles L, Mondieig D, Haget Y, Cuevas-Diarte MA. XXIth JEEP, Rouen, 1995:301.
[26] Denicolo I, Craievich AF, Doucet J. J Chem Phys 1984;80 (12) :6200.
[27] Jouti B, Provost E, Petitjean D, Bouroukba M, Dirand M. J Mol Struct 1996;382:49.
[28] Nouar H, Petitjean D, Bourdet JB, Bouroukba M, Dirand M. Thermochimica Acta 1997;293:87.
[29] Nouar H, Petitjean D, Bourdet JB, Dirand M. J Mol Struct 1998;443:197.
[30] Robles L, Mondieig D, Haget Y, Cuevas-diarte MA, Alcobe X. Mol Cryst Liq Cryst 1996;281:279.
[31] Clavell-Grunbaum D, Strauss HL, Snyder RG. J Phys Chem 1997;B101:335.
[32] King HE Jr., Sirota EB, Shao HH, Singer DM. J Phys D: Appl Phys 1993;B133:26.
[33] Sirota EB, King Jr HE, Singer DM, Shao HH. J Chem Phys 1993;98:5809.
[34] Robles L, Mondieig D, Haget Y, Cuevas-Diarte MA. J Chim Phys 1998;95:92.
[35] Craievich A, Doucet J, Denicolo I. J Physique 1984;45:1473.